

Theoretical and Computational Analyses of LNG Evaporator

Palani Kumar Chidambaram, Yang Myung Jo^{*}, Heuy Dong Kim^{*}

FMTRC, Daejoo Machinery Co Ltd, 149, Seongseodong-ro, Dalseo-Gu, Daegu 42721, Korea

^{*} Department Mechanical Engineering, Andong National University, 1375, Gyeongdong-ro, Andong-si, Gyeongsang-buk-do 760-749, Korea

© Science Press and Institute of Engineering Thermophysics, CAS and Springer-Verlag Berlin Heidelberg 2017

Theoretical and numerical analysis on the fluid flow and heat transfer inside a LNG evaporator is conducted in this work. Methane is used instead of LNG as the operating fluid. This is because; methane constitutes over 80% of natural gas. The analytical calculations are performed using simple mass and energy balance equations. The analytical calculations are made to assess the pressure and temperature variations in the steam tube. Multiphase numerical simulations are performed by solving the governing equations (basic flow equations of continuity, momentum and energy equations) in a portion of the evaporator domain consisting of a single steam pipe. The flow equations are solved along with equations of species transport. Multiphase modeling is incorporated using VOF method. Liquid methane is the primary phase. It vaporizes into the secondary phase gaseous methane. Steam is another secondary phase which flows through the heating coils. Turbulence is modeled by a two equation turbulence model. Both the theoretical and numerical predictions are seen to match well with each other. Further parametric studies are planned based on the current research.

Keywords: LNG Evaporator, Analytical Calculation, Numerical Simulation

Introduction

Liquefied Natural Gas, abbreviated as LNG is natural gas that is liquefied by refrigeration at its source. It is then usually transported via road or sea in large containers. LNG vaporizers are typically used for re-gasification of this LNG before it is transferred to a natural gas transportation pipeline. The vaporizers are basically heat exchangers which transfer heat from a hot fluid to LNG. The hot fluid varies depending on the kind of vaporizers. Some of the major types of evaporators are Open Rack Vaporizers (ORV), Submerged Combustion Vaporizers (SCV) and Intermediate Fluid Vaporizers (IFV) [1]. Each kind of vaporizer has its own benefits and limitations. The plant-specific selection of a vaporizer is made based upon several factors which include site location, availa-

bility of reliable heat source, environmental permissions and restrictions, demand and cost. Recently, a large number of LNG import terminals are shifting towards warmer climate equatorial regions where the IFVs are gaining importance [1]. Besides, IFVs are also superior over other vaporizers for transportable re-gasification units and waste heat recovery units [2]. Some recent investigations in the IFVs can be found in literature [2-5].

An IFV is a shell and tube type heat exchanger consisting of three prominent components: an evaporator, a condenser and a thermolator [2]. The evaporator contains high pressure steam tubes that are used to heat LNG. A typical evaporator is as shown in Fig. 1. LNG is fed into the evaporator through a porous media where it drips over the steam tubes. A part of heat from this super heated steam is transferred to LNG thereby vaporizing it

into gaseous NG. This gasified natural gas is collected through the outlet tube. Usually several layers of steam tubes located in the evaporator.

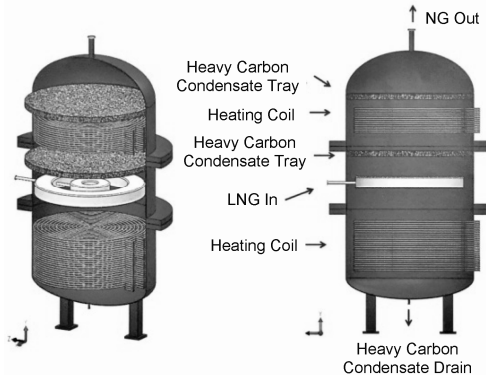


Fig. 1 Parts of an evaporator for LNG re-gasification

In the present work, for simplicity, only a portion of this evaporator is examined both theoretically and numerically. The analytical calculations are carried out to predict pressure and temperature variation in the steam tubes. Numerical simulations are also carried out to predict the flow field inside the evaporator. Various thermodynamic parameters like, pressure, temperature and velocity of LNG, evaporation rate of LNG, pressure, temperature and velocity of steam in the heating tubes are monitored and studied.

Parametric studies are planned for various arrangements of the heating coils like zig-zag, spiral etc. The ongoing research work focus on optimal arrangement of coils for uniform and efficient vaporization.

In the following sections, the theoretical predictions are discussed first. This is followed by discussions on the numerical simulations.

Theoretical method of solutions and results

Pipe flow - Prediction of pressure loss

Theoretical calculations for pressure loss in the pipe can be calculated using the classical Darcy-Weisbach equation. In SI units, the pressure drop can be rewritten [6] as follows.

$$\Delta P = \frac{f l v W^2}{D^5} \quad (1)$$

where f , l , v , W and D are Darcy friction factor extracted from Moody diagram, pipe length, specific volume of steam, steam flow rate in kg/hr and pipe diameter in mm .

For, pipes with bends, an equivalent length [6] can be added with the pipe length. In the present manuscript the design with zig-zag steam tube evaporator alone is discussed. The original length of the pipe is 10.6 m and

considering the pipe bends, the equivalent length of the pipe increases to 12.06 m. For the steam flow rate of 6.1 g/s through a single pipe at 433 K and 5 bar pressure through the pipe diameter of 12 mm, the Reynolds number of the flow is about 48121. For this Re, the friction factor from the Moody's diagram is 0.0202. Thus, the pressure drop calculated using the Eq. (1) is 11656.4 Pa.

Evaporator - Prediction of steam temperature drop

Then, analytical calculations in the evaporator is performed by writing a simple energy balance equation to calculate the temperature drop in the steam for a given flow rate and thermal conditions of liquid methane, steam and the gaseous methane at the outlet. The equation is as follows.

$$Q_S = Q_M \quad (2)$$

Here Q_S is the heat transferred from the steam and Q_M is the heat received by methane. The heat received by methane comprises of sensible heat rise of liquid methane up to its boiling point (Q_{LM}), latent heat of vaporization (L_{EV}) and sensible heat rise of gaseous methane (Q_{GM}) up to the required outlet temperature.

Thus,

$$Q_S = Q_{LM} + Q_{EV} + Q_{GM} \quad (3)$$

$$\Rightarrow \dot{m}_{ST} \int_{T_{OUT}}^{T_{IN}} C_{P_ST} dT = \dot{m}_{LM} \int_{T_{IN}}^{T_{OUT}} (C_{P_LM} dT) + \dot{m}_{EV} L_{EV} + \dot{m}_{GM} \int_{T_{IN}}^{T_{OUT}} (C_{P_GM} dT) \quad (4)$$

Here, the symbol \dot{m} , C_P , T , and L_{EV} stand for mass flow rate, specific heat capacity, temperature and latent heat of evaporation respectively. The subscripts ST , LM and GM indicate the properties of steam, liquid phase methane and gas phase methane respectively. Here the properties of methane are taken from [7] and the properties of steam are taken from NIST database. The boiling point of liquid methane [8] and the latent heat of vaporization of methane at the boiling point are taken from [9].

In the above Eq. (4), the mass flow rate of steam and liquid methane are given conditions. And, the inlet temperatures of both steam (433 K) and liquid methane (111 K) are given. The outlet temperature of gaseous methane and the mass of evaporation of liquid methane are taken from the CFD results which will be explained in the next section on numerical methods. This is done so as to ensure that Eq. 4 becomes a non-linear equation with a single unknown parameter - the outlet temperature of the steam. For a methane flow rate of 729 g/s and steam flow rate of 6.1 g/s and these conditions from CFD, the outlet temperature of steam is 289 K and thus the temperature drop of the steam is 144 K.

Evaporator - Prediction of heat transfer

To calculate heat transfer from the steam, the heat transfer coefficient on the inner walls of the tube is needed. This is calculated by the following Dittus-Boelter correlation for Nusselt number.

$$Nu = \frac{h_{in}d}{k} = 0.023 Re^{4/5} Pr^{0.3} \quad (5)$$

The Reynolds number (Re) inside the tube is 48300 for the given steam flow rate and pipe diameter. The Prandtl number (Pr) is 1.03. Hence, the Nusselt number (Nu) for the steam flow is calculated to be 129.8. And, the steam pipe internal heat transfer coefficient (h_{in}) that is calculated from Nusselt number is 282.29 W/(m².K).

For external flow over the tube, the Nu is calculated by the following Churchill-Bernstein equation.

$$Nu_D = \frac{h_{out}d}{k} = 0.3 + \frac{0.62 Re_D^{1/2} Pr^{1/3}}{\left[1 + (0.4/Pr)^{2/3}\right]^{1/4}} \left[1 + \left(\frac{Re_D}{282000}\right)^{5/8}\right]^{4/5} \quad (6)$$

In this relation, the pipe external Reynolds number (Re_D) is calculated based upon liquid methane flow rate and pipe diameter as 82.47. The Prandtl number (Pr) is 8.2, calculated based on liquid methane properties. Thus the Nusselt number (Nu_D) for the liquid methane flow is calculated to be 11.35. And the external heat transfer coefficient (h_{out}) is 31.42 W/(m².K). With inputs given for steam average temperature and liquid methane average temperature, the heat transfer on both sides of the steam tube walls can be compared to calculate average wall temperature and the heat transfer rate.

$$Q = h_{in}A(T_{ST} - T_W) = h_{out}A(T_W - T_{LM}) \quad (7)$$

The average values of steam temperature (T_{ST}) and liquid methane temperature (T_{LM}) are used in the above equation to find the only unknown wall temperature (T_W) which is calculated to be 339 K for evaporator.

Numerical method of solutions and results

Computational domain and mesh

For simplicity in the present numerical work, as explained earlier, only one row of the coils is chosen to be studied instead of choosing the whole evaporator. The computational domain is of 1050 mm in diameter, which is the model evaporator shell diameter. A heating coil of 12 mm in diameter and 10600 mm in length is located inside the evaporator. The coil is arranged in zig-zag fashion. The height of the evaporator section considered is 72 mm and the coil is located at 1/3rd height from the bottom. This location is selected to avoid occurrence of reverse flow in the numerical simulations.

Fig. 2 present the computational domain and the mesh

used in the simulations. High quality structured prismatic mesh was created inside the steam tube. An oval shaped tubular region around the coil is also created with structured mesh. The mesh was clustered towards the wall to resolve the momentum and thermal boundary layers. The smallest cell size in the wall normal direction was 0.025 mm. Unstructured tetrahedral mesh was created to cover the remaining domain. A few layers of prismatic were also provided near the inlet and outlet boundaries of LNG. The total mesh count in the domain was approximately 1 million cells.

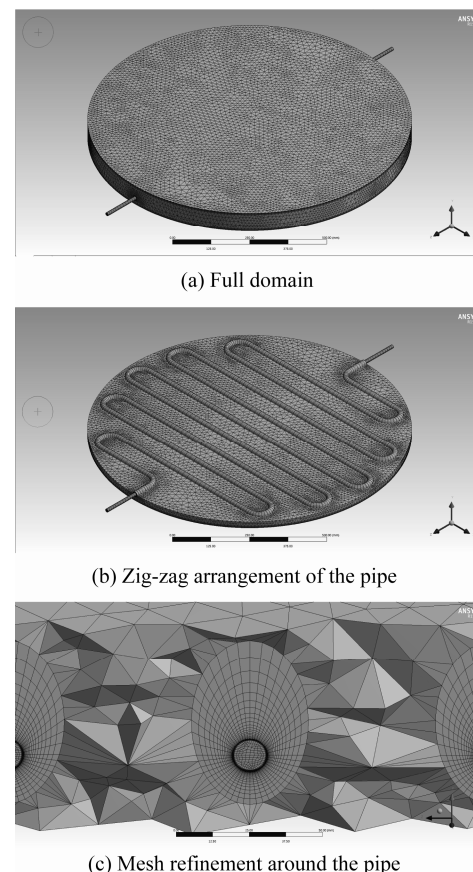


Fig. 2 Computational domain and mesh details

Cell zone and boundary conditions

The steam pipe is modeled as the fluid zone high pressure and temperature steam. The region around this pipe is the modeled as the fluid zone for methane flow. The bottom circular face of the evaporator tank is the inlet boundary for LNG with velocity inlet boundary condition. The top circular face is the outlet boundary for LNG with pressure outlet boundary condition. For the steam pipe, mass flow inlet and pressure outlet boundary conditions are provided. LNG is assumed to comprise of liquid methane, as methane is a predominant component, over 80% in the natural gas. The boundary condition of

liquid methane at the inlet are 111 K (-162°C) and 5.5 bar gauge pressure. The boundary condition for super-heated steam at the coil inlet are 433 K (160°C) and 5 bar gauge pressure.

Multiphase model

The complex flow occurring inside the evaporator is explained as follows. Hot steam flows through the pipe while liquid methane flows over the pipe. There is no mass transfer, but there is heat transfer from hot steam to cold liquid methane. Liquid methane absorbs this heat and then evaporates into gaseous methane. In the present numerical model this physical system is represented by a multiphase model containing three phases; steam, liquid phase methane and gas phase methane. In reality when the liquid methane vaporizes, bubbles will be formed at the steam pipe surface and get collected through the outlet pipe. The bubbles may vary on a wide range of diameters depending upon several physical parameters like surface roughness of the pipe, heat transfer rate, flow rate of steam and LNG etc. Accurate modeling of such bubbly flow requires very refined mesh throughout computational domain making it prohibitive in terms of the computational cost.

To solve this problem, an assumption is made to simplify the model that both the liquid and gas phase methane co-exist as interpenetrating media and both are continuous phases. Hence, the multiphase model needs to solve only one additional transport equation - volume fraction of the phases in addition to the original governing equations. This is achieved by the volume of fluid model (VOF model). The phase transfer between liquid and gaseous methane is achieved by the evaporation-condensation model which predicts the rate of evaporation based on the saturation temperature of the methane.

In the following sections in this manuscript, numerical results of flow through steam pipe alone is discussed first. This result is compared with the theoretical pressure drop calculations discussed earlier. This is then followed by multiphase simulations in the evaporator.

Numerical simulations in the steam pipe

Single phase numerical simulation was carried out initially in the pipe section alone with steam as the working fluid. The inlet flow rate of the steam was 6.1 g/s at 5 bar and at 433 K. The pressure drop contour inside the pipe for the simulation is shown below.

It is noticed that the simulated pressure drop is 11490.5 Pa, whereas the one predicted by the Darcy equation is 11656.4 Pa. This is within 2% of the theoretical equation. Next multiphase simulations were performed in the full computational domain with heat and mass transfer between the phases.

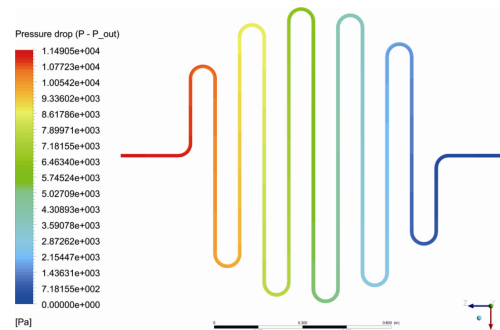


Fig. 3 Pressure drop contour in the steam pipe

Numerical simulations in the evaporator

Liquid methane is supplied at a velocity of 2 mm/s in the LNG inlet boundary that corresponds to a mass flow rate of about 729 g/s. Corresponding to the mass flow rate of 6.1 g/s, the inlet velocity of steam is 22 m/s. In an actual evaporator, multiple layers of steam pipes are used typically to ensure large flow rate of steam through the evaporator. Whereas, in the present simulations, only one layer of pipe is used to understand the flow and thermal pattern caused by the steam pipe.

The gaseous methane volume fraction and the temperature in the evaporator at various planes are presented in Fig. 4. One can note that the temperature of methane gas is higher near the periphery of the evaporator where the steam pipes bend and lower in the centre of the evaporator where the steam pipes run parallel to each other.

Fig. 5 shows the mass transfer rate contour indicating the phase transfer from liquid methane to gaseous methane. It is noticed that the phase transfer is restricted to a very small region around the steam tube. A volumetric integral of this mass transfer rate over the domain quantifies the total mass of liquid methane evaporated. For the given conditions, the simulations predicted 1.39 g/s of liquid methane evaporation and the mass averaged temperature at the exit of the evaporator was 111.7 K. Using these values in Eqs. (4) - (7), the steam temperature at the exit, the steam tube average wall temperature and the total heat transferred are calculated. As shown in Table 1, the theoretical and the numerical predictions match well.

Also, gaseous methane seems to be present only along the steam pipe length. The liquid methane escaping in between the steam pipes without coming in proximity seems to be leaving the domain unaffected. This is caused by the use of only one steam pipe and the shortage of steam flow rate to heat and convert the liquid methane into gas.

The pressure and temperature of the steam in the evaporator are presented in Fig. 6. It is interesting to note that the pressure drop has reduced from 11490.5 Pa in the first simulation with steam pipe alone to 10356.3 Pa here. This is caused by the heat loss to the liquid methane. A decrease in steam temperature causes a corresponding

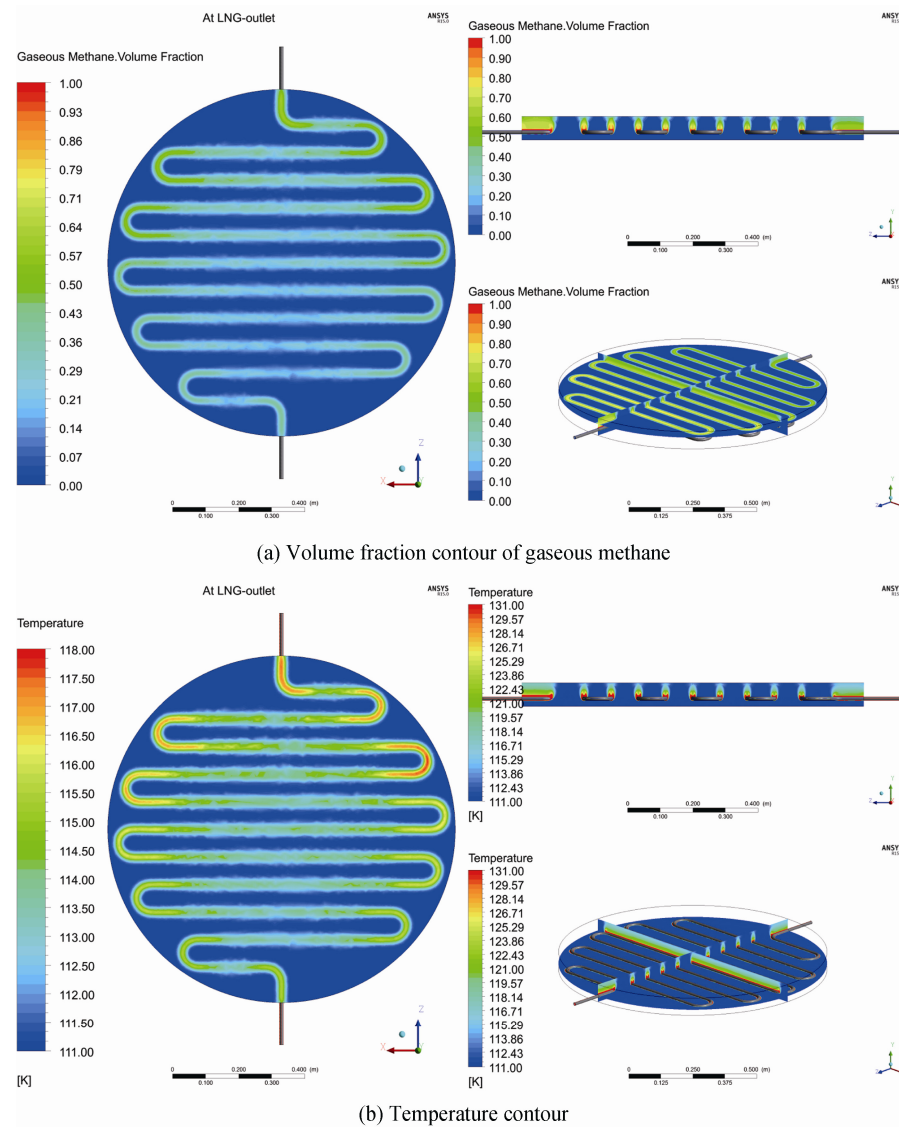


Fig. 4 Results of evaporator simulation

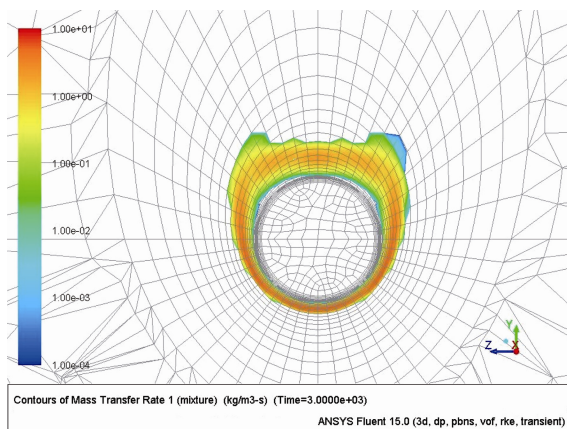


Fig. 5 Mass transfer rate contour around the steam tube

Table 1 Comparison of theoretical and numerical predictions

	Theoretical	CFD
Pressure drop (Pa)	11656.4	11490
Exit steam temperature (K)	289	287.3
Total heat transferred rate (W)	1778.2	1788.9
Steam tube average wall temperature (K)	339.1	339
Mass of methane evaporated (g/s)	1.39	
Mass-averaged LNG outlet temperature (K)	111.7	

decrease in its velocity and an increase in its density. Basic fluid mechanics states that the pressure drop varies as density and as square of velocity. Hence, the reduction in velocity is dominant than the increase in density. Therefore, the pressure drop in the steam pipe has reduced.

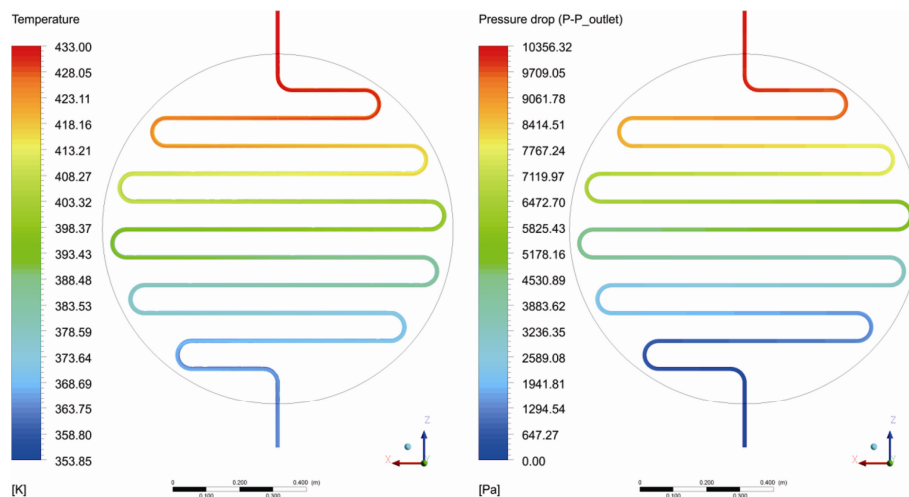


Fig. 6 Pressure and temperature contour inside the steam pipe in the evaporator

chinaXiv:201703.01045v1

Conclusions and future directions of the research work

In this manuscript, the physical processes in a typical LNG evaporator are analyzed by using both analytical equations and numerical simulations. The analytical calculations made use of theoretical equations based on simplified heat and mass balance equations to predict steam pressure and temperature drop. The numerical simulations were performed on a segment of the evaporator. Based on the study the following conclusions can be made.

A multiphase numerical model can be successfully applied for the prediction of physical processes inside a LNG evaporator. Comparisons of pressure drop and temperature drop in the steam were made between both predictions and they were found to match reasonably well.

Numerical simulation with the zig-zag arrangement of steam pipe shows non-uniform vaporization occurring in the evaporator. The vaporization rate and the temperature are higher around the periphery of the evaporator due to the presence of steam pipe bends and lower in the centre where they run parallel to each other.

Ongoing research focuses on modification of steam pipe design into a spiral pattern and further parametric studies on multiple steam pipes. It will be interesting to simulate and analyze the flow pattern in the evaporator with steam tubes of various patterns.

Acknowledgement

This work was supported by a grant from 2016 Research Funds of Andong National University.

References

- [1] Patel, D., Mak, J., Rivera, D. and Angtuaco, J., 2013. LNG vaporizer selection based on site ambient conditions. *Proceedings of the LNG*, 17, pp.16–19.
- [2] Xu, S., Chen, X. and Fan, Z., 2016. Thermal design of intermediate fluid vaporizer for subcritical liquefied natural gas. *Journal of Natural Gas Science and Engineering*, 32, pp.10–19.
- [3] Fengxia, L., Yuqiang, D., Wei, W., Jiupeng, Z., Che, Z., Chao, D. and Dapeng, H., 2013. Feasibility of intermediate fluid vaporizer with spiral wound tubes. *China Petroleum Processing & Petrochemical Technology*, 15(1), pp.73–77.
- [4] Pu, L., Qu, Z., Bai, Y., Qi, D., Song, K. and Yi, P., 2014. Thermal performance analysis of intermediate fluid vaporizer for liquefied natural gas. *Applied thermal engineering*, 65(1), pp.564–574.
- [5] Xu, S., Cheng, Q., Zhuang, L., Tang, B., Ren, Q. and Zhang, X., 2015. LNG vaporizers using various refrigerants as intermediate fluid: Comparison of the required heat transfer area. *Journal of Natural Gas Science and Engineering*, 25, pp.1–9.
- [6] Menon, S., 2004. *Piping calculations manual*. McGraw Hill Professional.
- [7] Younglove, B.A. and Ely, J.F., 1987. Thermophysical properties of fluids. II. Methane, ethane, propane, isobutane, and normal butane. *Journal of Physical and Chemical Reference Data*, 16(4), pp.577–798.
- [8] Speight, J.G., 2005. *Lange's handbook of chemistry*. New York: McGraw-Hill.
- [9] Hestermann, P. and White, D., 1961. The vapor pressure, heat of vaporization and heat capacity of methane from the boiling point to the critical temperature. *The Journal of Physical Chemistry*, 65(2), pp.362–365.